Materials Chemistry and Physics 204 (2018) 163–170

Contents lists available at ScienceDirect

Materials Chemistry and Physics

journal homepage: www.elsevier.com/locate/matchemphys

Diversified electrical properties of $(1-x)Ba_{0.90}Ca_{0.10}Ti_{0.95}Zr_{0.05}O_3-(x)RuO_2$ ceramics with defect electron complexes

Yongshang Tian [a, *], Shuiyun Li [a], Yansheng Gong [b], Yongsheng Yu [a], Yitian Tang [a], Peng Liu [a], Qiangshan Jing [a]

[a] Henan Province Key Laboratory of Utilization of Non–metallic Mineral in the South of Henan, College of Chemistry and Chemical Engineering, Xinyang Normal University, Xinyang 464000, People's Republic of China
[b] Faculty of Material Science and Chemistry, China University of Geosciences, Wuhan 430074, People's Republic of China

HIGHLIGHTS

- BCZT–xRu lead-free ceramics were prepared by a modified Pechini method.
- The phase evolution could be induced by a little addition of RuO_2 contents.
- RuO_2 was benefited for elevating electrical properties of the ceramics.
- The mechanism of defect electron complexes was sated in detail.
- Ferroelectric properties could be optimized by polarized–aged process.

ARTICLE INFO

Article history:
Received 18 August 2017
Received in revised form
18 September 2017
Accepted 12 October 2017

Keywords:
RuO_2-doped
BCZT-based ceramics
Phase evolution
Defect electron complexes
Ferroelectric properties

ABSTRACT

Lead-free $(1-x)Ba_{0.90}Ca_{0.10}Ti_{0.95}Zr_{0.05}O_3-(x)RuO_2$ (x = 0–2.0 mol%) ceramics were prepared by conventional solid state reaction with the as-synthesized nanoparticles by a modified Pechini method, showing high densification (96.4–97.1%) with the grain size of ~2.2 μm. Effects of RuO_2 contents on the ceramics crystal structure and electrical properties were investigated. The phase evolution was identified by X-ray powder diffraction analysis, and the coexisted Tetragonal and Rhombohedral phases were detected at x around 1.0 mol%. The formation mechanism of defect electron complexes was sated in detail. Diversified dielectric properties and ferroelectric relaxation stemmed from defect electron complexes, charge accumulation at grain boundary, long-range ferroelectric dipole order, etc. Ferroelectric properties could be optimized apparently by polarized–aged process. The optimum electrical properties, i.e. d_{33} = 195 pC/N, k_p = ~0.22, and Q_m = 78.9, were obtained at x = 1.0 mol%.

1. Introduction

Piezoelectric devices can convert mechanical energy to electrical energy and vice-versa, and the functional application includes actuators, pyroelectric devices, sensors, etc. [1,2] Lead-free piezoelectric materials have been extensively researched for alternating lead-based materials as the requirements of developing eco-friendly materials in the past decades [3]. Currently, lead-free candidates, i.e., $BaTiO_3$ (BT), $K_{0.5}Na_{0.5}NbO_3$ (KNN), $Bi_{0.5}Na_{0.5}TiO_3$ (BNT), and $BiFeO_3$ (BF)-based materials systems, show considerable piezoelectric properties because of the perovskite (ABO_3) structure with specific phase morphology (polymorphic phase transition, PPT; or morphotropic phase boundary, MPB) by doping or substituting other elements [4–7]. Among the candidates, calcium and zirconate co-doped barium titanate (BCZT)-based ceramic materials feature high piezoelectric properties, controllable sinterability, and excellent thermostability, regarding as the promising materials and receiving tremendous worldwide attentions [8,9].

In recent years, lead-free BCZT-based ceramics were optimized by doping rare-earth elements, adding low temperature eutectic mixtures, modifying sintering process, etc. for overcoming the flaws and obtaining excellent multifunctional performance

* Corresponding author. College of Chemistry and Chemical Engineering, Xinyang Normal University, Xinyang 464000, People's Republic of China.
E-mail addresses: tianyongshang423@163.com, tianyongshang@xynu.edu.cn (Y. Tian).

https://doi.org/10.1016/j.matchemphys.2017.10.038
0254-0584/

[10–12]. The platinum group element iridium doped BCZT-based ceramics were studied in our previous research, indicating good electrical properties that could be used in electrode buffer layer in multilayer ceramic capacitors (MLCCs) [13]. However, the other platinum group element ruthenium (Ru)-doped BCZT-based ceramics were seldom reported, which might have potential application in microelectronic devices, electrodes, and catalyst [14,15]. It was reported that the polarization rotation and extension were responsible for elevating electrical properties [16]. And the nanoscale piezoelectric domains formed in the preparing process, which could influence on the polarization alignment and the ferroelectric properties [17]. Thus, finding and surmounting the differences among virgin and polarized–aged BCZT-based ceramics are vital for the stable ferroelectric properties and piezoelectric devices.

The defect electron complexes and point defects play a significant role on tailoring piezoelectric materials [18]. Particularly, the defect electron complexes between the dimeric acceptor dopant ions and charge are generated for compensating oxygen vacancy due to charge balance, which have pronounced the important impact on the electrical properties [18,19]. However, the mechanism of defect electron complexes of RuO_2 doped BCZT-based ceramics on the electrical properties was rarely reported before. In this work, RuO_2 doped $(1-x)Ba_{0.90}Ca_{0.10}Ti_{0.95}Zr_{0.05}O_3-(x)RuO_2$ (x = 0–2.0 mol%) lead-free ceramics were sintered at a low temperature of 1240 °C by conventional solid state reaction with the as-prepared nanoparticles which were prepared by a modified Pechini method [20]. The influence on the crystal structures and electrical properties as a function of doping various RuO_2 contents were systematically investigated. The origin of phase evolution, ferroelectric relaxor behavior, dielectric dispersion, diffuse phase transition, ferroelectricity, and piezoelectricity of the ceramics that influenced by the addition of RuO_2 contents were studied in detail. Moreover, the formation mechanism of defect electron complexes and the reason of optimized ferroelectric properties by polarized–aged process were explored.

2. Experimental

$(1-x)Ba_{0.90}Ca_{0.10}Ti_{0.95}Zr_{0.05}O_3-(x)RuO_2$ (abbreviated as BCZT–xRu; x = 0, 0.5, 1.0, 1.5, and 2.0 mol%) ceramics were prepared by conventional solid state reaction under a low sintered temperature with as-synthesized nanoparticles. The BCZT nanoparticles were prepared by a modified Pechini polymeric precursor method as we had reported, using $Ti(OC_4H_9)_4$, $Zr(NO_3)_4$, $Ca(NO_3)_2$, $Ba(CH_3COO)_2$, ethylene glycol monomethyl ether, and citric acid [20,21]. The starting materials of BCZT nanoparticles and RuO_2 nanoparticles were homogeneously mixed with 2.5 wt% polyvinyl alcohol solution as binder, and then uniaxially pressed into a discs of 20 mm in diameter and ~1.5 mm in thickness under 150 MPa. The binder was burnt out at 670 °C for 2 h in air at porcelain boat first, and then the green samples were buried in Al_2O_3 powders and were sintered at 1240 °C for 6 h in air atmosphere. The silver pastes were applied on the surfaces of the both polished discs sides as electrodes for the subsequent electrical measurements. Then, the samples were polarized in silicone oil bath at 25 °C for 30 min by applying a direct–current electric field of 15 kV/cm.

Crystal phases of the ceramics were investigated by X-ray powder diffraction (XRD; X'Pert PRO) at a 2θ scanning rate of 0.05°/s. The crystal structure, symmetry, and structure defects of the ceramics were analyzed by Raman spectroscopy (Horiba Jobin Yvon) that speculated at room temperature. The densification of the ceramics was calculated with Archimedes immersion principle by precision electronic balance (ES-220D). The fractured microstructures of the ceramics were investigated by scanning electron microscope (SEM; S4800). The relative permittivity (ε_r) and loss tangent (tan δ) of the ceramics from room temperature to 175 °C under different frequency were tested by dielectric measurement system (HDMS-1000 V). A radiant precision workstation (PRE-MERII) was carried to measure polarization–electric field (P–E) hysteresis loops. A precision impedance analyzer (Keysight-4990A) was carried to investigate the planar vibration electromechanical coupling (k_p) and mechanical quality (Q_m) factors. Piezoelectric constant (d_{33}) was measured by a quasistatic piezoelectric constant testing meter (ZJ-3AN) at room temperature.

3. Results and discussion

Fig. 1 shows the XRD patterns and phase evolution of BCZT–xRu ceramics with RuO_2 contents of 0, 0.5, 1.0, 1.5, and 2.0 mol%. It could be seen the diffraction peaks were intensive fierceness under the test condition, indicating a high crystallinity of the ceramics. The pure perovskite structure (ABO_3) without secondary phases of the samples suggested ruthenium diffused into the crystal lattice successfully. From selected enlarged region in Fig. 1b, the unique splitted $(002)^T$ and $(200)^T$ diffraction peaks of Tetragonal (T) phase (JCPDS # 05-0626) appeared when x < 0.5 mol%, the peaks changed into $(200)^R$ diffraction peak of Rhombohedral (R) phase (JCPDS # 85-1796) with further increased RuO_2 contents, and the coexisted T and R phase regions of the ceramics were found at x around 1.0 mol %, showing ruthenium would induce the phase evolution of the ceramics [22]. What's more, the diffraction peaks subtly shifted to a high 2θ angle monotonically with increasing RuO_2 contents, because of the decreased interplanar crystal spacing as the replacement of ionic radius Ba^{2+} (0.161 nm), Ca^{2+} (0.134 nm), or Zr^{4+} (0.074 nm) by the smaller Ru^{4+} (0.067 nm) in the structure [23]. Additionally, the excessive RuO_2 contents doping might give rise to the structure defect and lattice stress, which leaded to deteriorated electrical properties of the ceramics.

Fig. 2a and Fig. 2b show the Rietveld refinement XRD patterns of BCZT–xRu ceramics with RuO_2 contents of 0 and 1.5 mol%, which were refined by considering $P4mm$ and $R3m$ space group, respectively. From Fig. 2a and b, the detected experimental XRD pattern peak positions fitted well with the model Bragg positions, and the fitting parameters in Fig. 2a (R_p = 8.67, R_{wp} = 10.31, and χ^2 = 1.97) and Fig. 2b (R_p = 9.58, R_{wp} = 12.13, and χ^2 = 2.21) indicated the calculated XRD patterns were highly consistent with the detected

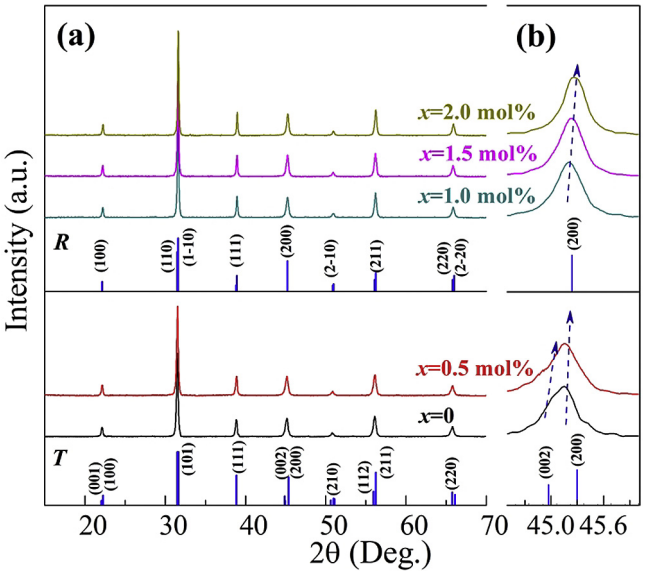

Fig. 1. (a) XRD patterns and (b) corresponding selected enlarged regions (44.1–46.5°) of the BCZT–xRu ceramics with varying RuO_2 contents (x).